

Magnetic Transitions in K-Doped Biphenyl and *p*-Terphenyl

Guo-Hua Zhong¹, Chao Zhang², Ming Chen¹, Xiao-Jia Chen³, and Hai-Qing Lin⁴

HPSTAR
616-2018

¹Shenzhen Institutes of Advanced Technology, Chinese Academy of Sciences, Shenzhen 518055, China

²Department of Physics, Yantai University, Yantai 264005, China

³Center for High Pressure Science and Technology Advanced Research, Shanghai 201203, China

⁴Beijing Computational Science Research Center, Beijing 100193, China

Recently, an interesting superconductivity of the transition temperatures range from 7.2 to 43 K and then to 123 K in K-doped *p*-terphenyl was reported, which attracts much attention. In this paper, to identify the superconducting phase from chemical component, we have investigated the crystal structures and electronic and magnetic properties in the cases of K-doped biphenyl and *p*-terphenyl based on the first-principles calculations. We found that the change of doping concentration results in a series of magnetic transitions. Pristine biphenyl and *p*-terphenyl are both nonmagnetic (NM) semiconductors. Doping one K atom for each organic molecule, the system exhibits the antiferromagnetism. With increasing the doping concentration of K atoms, however, the spin ordering disappears and the compound behaviors as the NM metal. Thus, we suggest that the superconducting phases observed experimentally are corresponding to the highly doping levels, which will deepen the understanding of the superconductivity of aromatic hydrocarbons.

Index Terms—Antiferromagnetism, biphenyl, electronic structures, magnetism, superconductivity, terphenyl.

I. INTRODUCTION

BASED on the idea of that the interaction of electrons with much higher excitation energy than the phonon energy can result in a substantially higher T_c , the organic materials were believed as candidates of high-temperature or room-temperature superconductors [1], [2]. In 2010, the discovery of superconductivity with $T_c \sim 18$ K in potassium (K)-doped picene accelerated the research of organic superconductors [3]. Subsequently, several aromatic hydrocarbon superconductors, such as K-doped phenanthrene, coronene, and 1,2;8,9-dibenzopentacene, were also reported [4]–[6]. Among those systems, the highest T_c is only 33.1 K [6] which was far from the room-temperature superconductor. Recently, however, the interesting superconductivity in potassium-doped *p*-terphenyl ($K_xC_{18}H_{14}$) has been discovered by Wang *et al.* [7]–[9], with an amazing change of superconducting critical temperature from 7.2 to 43 K and then to 123 K. A superconducting gaplike feature persisting to 60 K or above was observed in $K_xC_{18}H_{14}$ by measurements of angle resolved photoemission spectroscopy [10]. Furthermore, the magnetization measured by Liu *et al.* [11] confirmed the superconductivitylike transition at about 125 K. The remarkable superconductivity of phenyl-like aromatic hydrocarbons has attracted much attention. First, the chemical component of the superconducting phase is an urgent need for researchers to know. Inevitably, magnetism is also well worth studying in such materials to understand the superconducting mechanism.

In our previous study on K-doped picene [12], we have pointed out that the magnetism is high sensitive to the system volume. Starting from the volume generated by experimental lattice constants, the compressing volume makes the

system stabilize at a nonmagnetic (NM) state, while the expanding volume results in the enhancement of antiferromagnetic (AFM) character. For the system containing different numbers and arrangements of benzene rings, such as phenanthrene, picene, 1,2;5,6-dibenzanthracene, 7-phenacene, and 1,2;8,9-dibenzopentacene, we found that these optimized structures are stabilized at the AFM state [13]. Especially, the AFM spin moment is in direct proportion to the number of C atoms in system and independent on the arrangement of benzene rings. In K-doped aromatic compounds, the magnetism almost all originates from C atoms, while K atom does not contribute to the magnetism. In Sm-doped phenanthrene and chrysene [14], [15], on the contrary, Sm induces the bigger local magnetic moment comparing with C atoms, in which the strong magnetic correlation has not the positive contribution to the superconductivity. Most recently, Takabayashi *et al.* [16] observed the spin-liquid behavior in Cs_1 phenanthrene and the diamagnetic phenomenon in Cs_2 phenanthrene.

Thus, it can be seen that doped aromatic compounds exhibit rich magnetism except for superconductivity. However, *p*-terphenyl, as well as biphenyl ($C_{12}H_{10}$), is non-edge-shared aromatic compound, different from picene, phenanthrene, and 1,2;8,9-dibenzopentacene. Then, what about the magnetism of K-doped biphenyl and *p*-terphenyl? In our previous studies mentioned earlier, all of the K contents in those systems are fixed at $x \sim 3$, which was mentioned by experiments. What will happen when the doping concentration is changed? To answer these questions, we have analyzed the crystal and electronic and magnetic properties of $C_{12}H_{10}$ and $C_{18}H_{14}$, respectively, containing different K contents based on the first-principles calculations.

II. COMPUTATIONAL METHODS

The structural, electronic, and magnetic characteristics of $K_xC_{12}H_{10}$ and $K_xC_{18}H_{14}$ were systematically investigated by using the generalized gradient approximation (GGA) [17] plus

Manuscript received December 19, 2017; accepted June 11, 2018. Date of publication July 6, 2018; date of current version August 17, 2018. Corresponding author: G.-H. Zhong (e-mail: gh.zhong@siat.ac.cn).

Color versions of one or more of the figures in this paper are available online at <http://ieeexplore.ieee.org>.

Digital Object Identifier 10.1109/TMAG.2018.2847686

0018-9464 © 2018 IEEE. Personal use is permitted, but republication/redistribution requires IEEE permission.

See http://www.ieee.org/publications_standards/publications/rights/index.html for more information.

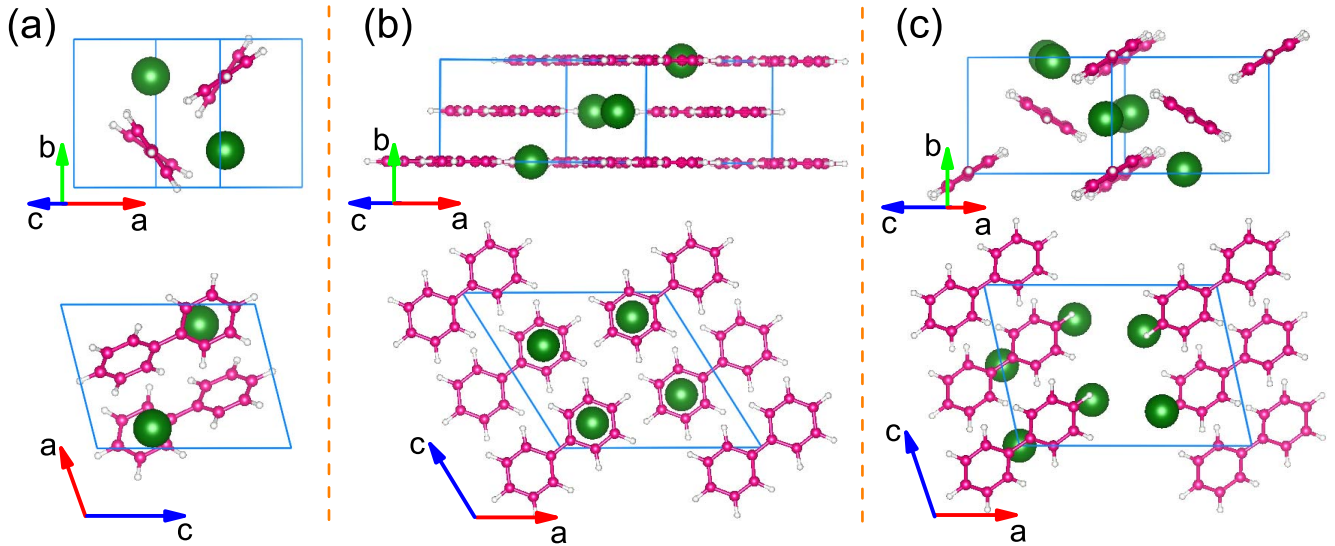


Fig. 1. Crystal structures of $K_xC_{12}H_{10}$ viewing from different directions. Green spheres represent K atoms. (a)–(c) $K_1C_{12}H_{10}$, $K_2C_{12}H_{10}$, and $K_3C_{12}H_{10}$, respectively.

TABLE I
OPTIMIZED CRYSTAL LATTICE PARAMETERS OF PRISTINE AND K-DOPED BIPHENYL BASED ON vdW-DF2 FUNCTIONAL

System	Space-group	a (Å)	b (Å)	c (Å)	β (°)	V (Å ³)
$C_{12}H_{10}$	$P2_1/c$	11.862	5.532	7.965	127.6	414.0
$K_1C_{12}H_{10}$	$P2_1$	7.193	7.142	9.411	104.06	469.1
$K_2C_{12}H_{10}$	$P2_1/c$	11.445	5.473	10.468	122.99	550.1
$K_3C_{12}H_{10}$	$P2_1/c$	12.755	6.099	9.032	102.47	686.1

van der Waals (vdW) [18] corrections implemented in the Vienna Ab-initio simulation package [19], [20]. The cutoff energy for plane wave basis was set as 600 eV. All the optimizations were performed using the conjugate-gradient algorithm. The Monkhorst–Pack k -point grids were generated according to the specified k -point separation 0.04 \AA^{-1} for relaxation and 0.02 \AA^{-1} for self-consistency calculation. The convergence thresholds were set as 10^{-6} eV in energy and 5×10^{-3} eV/Å in force.

III. RESULTS AND DISCUSSION

Our previous studies [14], [15], [21], [22] have confirmed that the GGA plus vdW correction in vdW-DF2 version [18] can accurately predict the crystal lattice parameters of aromatic hydrocarbons. Changing the K contents in this paper, therefore, we fully optimized the doped structures including the lattice constants and atomic positions. Crystal structures and lattice parameters of $K_xC_{18}H_{14}$ have been reported in our previous work [23]. In this paper, we emphasize the crystal structures and lattice parameters of $K_xC_{12}H_{10}$. Considering three doping contents of $x = 1, 2,$ and 3 , we searched the optimal structures in several possible space groups. For each doping concentration, we selected the structure with the lowest energy to show in Fig. 1 and list the crystal lattice parameters in Table I, respectively. Although the doped compounds display different space groups, there are two aromatic molecules in each unit cell. The intercalating K atoms into biphenyl and p -terphenyl crystal both make the volume expand. The variations of K contents lead to the visible difference of the

crystal configuration. The stable $K_1C_{12}H_{10}$ and $K_1C_{18}H_{14}$ show the non-coplanar features of benzene rings. There is a tilted angle between two successive benzene rings with respect to each other. Under other two doping concentrations, the benzene rings in aromatic molecule are coplanar. Especially, the pure 2-D structure was observed in the K-doped case, corresponding to $K_2C_{12}H_{10}$ and $K_3C_{18}H_{14}$ [23], respectively.

Starting from the crystal structures obtained, the magnetic ground states were determined by calculating the total energy under the NM, FM, and AFM states. Referred from our previous studies [12], [13], the AFM spin polarization was set as parallel within the same molecule and antiparallel between the molecules. The calculated total energies relative to the lowest energy are summarized in Table II. Pure biphenyl and p -terphenyl (no doping) are both the NM semiconductor with the big bandgap (E_g) of 3.09 and 2.61 eV, respectively. The long-range magnetic ordering does not exist in these pure phases. After doping, similar to K-doped edge-shared cases, such as phenanthrene, picene, and 1,2;8,9-dibenzopentacene [13], the FM behavior does not exist in $K_xC_{12}H_{10}$ or $K_xC_{18}H_{14}$, since the initial FM polarization is quenched by the electronic relaxation. As shown in Table II, both $K_1C_{12}H_{10}$ and $K_1C_{18}H_{14}$ are stabilized at the AFM ground state. Fig. 2 shows the spin densities of $K_1C_{12}H_{10}$ and $K_1C_{18}H_{14}$. The AFM spin ordering is visibly observed among the molecules. The result means that the introduction of K atoms caused the transition from NM to AFM. At the same time, the spin density mainly concentrates on C atoms, which indicates that K and H atoms do not contribute to

TABLE II

TOTAL ENERGIES UNDER DIFFERENT MAGNETIC STATES RELATIVE TO THE LOWEST ENERGY. M REPRESENTS THE LOCAL SPIN MOMENT FOR AFM GROUND STATE. E_g IS THE BANDGAP OF THE SYSTEM AT ITS MAGNETIC GROUND STATE. $N(E_F)$ IS THE DOS AT THE FERMI LEVEL

System	NM (meV/f.u.)	FM (meV/f.u.)	AFM (meV/f.u.)	M (μ_B /f.u.)	E_g (eV)	$N(E_F)$ (states/eV/f.u.)
$C_{12}H_{10}$	0	none	none	0	3.09	0
$K_1C_{12}H_{10}$	21.0	none	0	0.49	0	0
$K_2C_{12}H_{10}$	0	none	none	0	0	0.47
$K_3C_{12}H_{10}$	0	none	none	0	0	3.08
$C_{18}H_{14}$	0	none	none	0	2.61	0
$K_1C_{18}H_{14}$	20.2	none	0	0.57	0	0
$K_2C_{18}H_{14}$	0	none	none	0	0	1.28
$K_3C_{18}H_{14}$	0	none	none	0	0	3.57

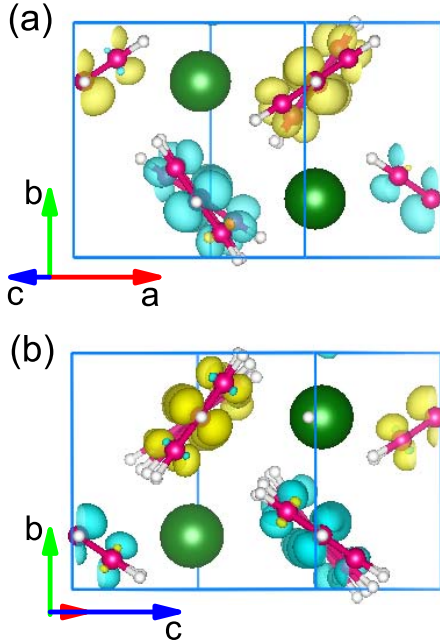


Fig. 2. Calculated spin densities of (a) $K_1C_{12}H_{10}$ and (b) $K_1C_{18}H_{14}$. The different colors of electronic clouds represent the difference of spin directions. Iso-surface unit: $3 \times 10^{-3} e/\text{\AA}^3$.

the AFM magnetic moment. Comparing the special structural characteristic shown in Fig. 1 and presented in [22], we infer that the tilting between two successive benzene rings drives the AFM spin ordering of electrons transferred to C atoms from K atoms. When the doping concentration $x \geq 2$, as shown in Table II, both the FM and AFM spin polarizations are quenched after the electronic relaxation. Namely, the doped system with $x \geq 2$ exhibits the NM behavior. Thus, another magnetic transition from AFM to NM was observed at $x = 2$ for $K_xC_{12}H_{10}$ and $K_xC_{18}H_{14}$. As the doping concentration increasing to $x = 3$ from $x = 2$, no magnetic transition is occurred.

In Cs_1 phenanthrene [16], the $P2_12_12_1$ symmetry made phenanthrene molecules arrange an approximate triangle along the c -direction. The strong spin fluctuation formed the spin-liquid state in Cs_1 phenanthrene, while in Cs_2 phenanthrene [16] with the $P2_1/a$ symmetry, the herringbone packing was also abandoned, which leads to the diamagnetism. The results from Takabayashi *et al.* [16] imply an importance of organic molecular configuration to magnetism. In this paper, for these two magnetic phase transitions mentioned earlier (respectively, at $x = 1$ and $x = 2$) induced by doping, we point out that it is relation to the

crystal configuration. Based our structural optimization, all of the benzene rings in every organic molecule are coplanar in the optimized structures of pristine $C_{12}H_{10}$ and $C_{18}H_{14}$. But doping one K atom for each organic molecule ($x = 1$), as reported in [22] and shown in Fig. 1, the K atom is at one end of the molecule which results in the existence of tilting angle between the two successive benzene rings. Extending the calculation to the doping concentration of $x = 1.5$, we also observed the tilting between two successive benzene rings as well as the AFM behavior. However, when $x \geq 2$, the K atoms are symmetrically distributed on the molecular plane viewing along the direction perpendicular to the plane. Therefore, the crystal structures go back to the coplanar characteristics again at the doping concentration $x = 2$ and keep it to $x = 3$. Based on this point, we infer that the magnetic phase transitions come from the structural variations induced by doping. For the AFM $K_1C_{12}H_{10}$ and $K_1C_{18}H_{14}$, the local spin moment reaches to $0.49 \mu_B$ /f.u. and $0.57 \mu_B$ /f.u., respectively. In the previous study [13], we have reported that the local spin moment is dependent on the number of C atoms. For instance, the local spin moments of the AFM states of K-doped phenanthrene, picene, and 1,2;8,9-dibenzopentacene are in the magnitudes of $0.3 \mu_B$ /f.u., $0.4 \mu_B$ /f.u., and $0.5 \mu_B$ /f.u., respectively. The magnetic moment increases with the number of C atoms, which reappears in $K_1C_{12}H_{10}$ ($0.49 \mu_B$ /f.u.) and $K_1C_{18}H_{14}$ ($0.57 \mu_B$ /f.u.). Comparing these two kinds of aromatic hydrocarbons combing with the different of the number of C atoms, we can conclude that the spin moments in non-edge-shared $K_xC_{12}H_{10}$ and $K_xC_{18}H_{14}$ are bigger. However, when C atoms further increasing, the spin magnetic moment could be improved to more than 1 Bohr magneton, such as $1.5 \mu_B$ /f.u.– $3.5 \mu_B$ in armchair graphene nanoribbons [24].

Based on these magnetic ground states, we have calculated the density of states (DOS) of $K_xC_{12}H_{10}$ and $K_xC_{18}H_{14}$ and shown in Fig. 3. Comparing with pristine biphenyl and *p*-terphenyl, the charge transferring to C atoms from K atoms leads to the shift of the Fermi level toward to higher energy. The electronic states near the Fermi level are mainly contributed by 2p electrons of C atoms. Under the AFM polarization, the Fermi level almost lies in the pseudoenergy gap in $K_1C_{12}H_{10}$ and $K_1C_{18}H_{14}$. The electronic state at the Fermi level is lack. Therefore, we ascertain that the superconductivity cannot occur in these AFM phases of $K_1C_{12}H_{10}$ and $K_1C_{18}H_{14}$. Under the even numbered doping such as $x = 2$, the DOS at the Fermi level [$N(E_F)$] is small, about 0.47 states/eV/f.u. for $K_2C_{12}H_{10}$ and 1.28 states/eV/f.u.

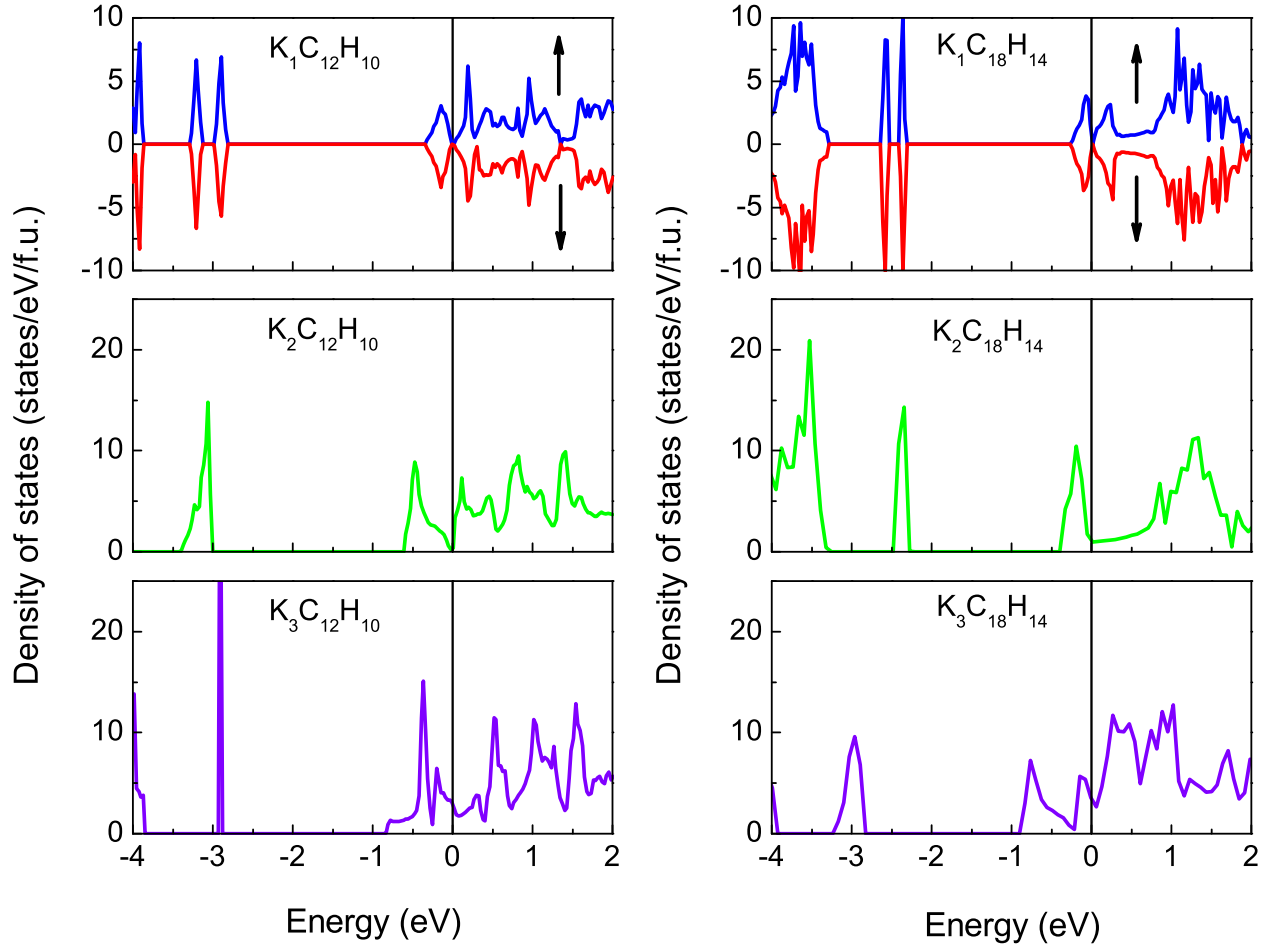


Fig. 3. DOS of $K_xC_{12}H_{10}$ and $K_xC_{18}H_{14}$ are presented. For $K_1C_{12}H_{10}$ and $K_1C_{18}H_{14}$, the AFM spin polarization is distinguished as spin up (\uparrow) and spin down (\downarrow), respectively. For other doping levels, the NM DOS are plotted.

for $K_2C_{18}H_{14}$ as listed in Table II. So, they exhibit the weak metallicity. Further increasing electrons into the system, the Fermi level shifts toward to higher energy and the $N(E_F)$ value becomes big. To $x = 3$, the $N(E_F)$ is, respectively, 3.08 and 3.57 states/eV/f.u. for $K_3C_{12}H_{10}$ and $K_3C_{18}H_{14}$. Since both $K_xC_{12}H_{10}$ and $K_xC_{18}H_{14}$ are NM metals as the doping concentration from $x = 2$ to $x = 3$, then we suggest that the superconducting phases observed by experiments are just corresponding to the doping concentration in the range of $2 \leq x \leq 3$ for $K_xC_{12}H_{10}$ and $K_xC_{18}H_{14}$. Moreover, the difference of doping concentration will drive the superconducting transition temperature to change. However, for the broad superconducting critical temperature of T_c from 7.2 to 43 K and then to 123 K experimentally observed in $K_xC_{18}H_{14}$, we suppose the existence of other superconducting modes, such as C_{60} and KH_x , except for the difference of doping levels.

IV. CONCLUSION

In this paper, we have investigated the crystal structures and electronic and magnetic properties of K-doped biphenyl and *p*-terphenyl by the first-principles calculations. When doping one K atom for each organic molecule into pristine system, seen from the systemic energy, both $K_1C_{12}H_{10}$ and $K_1C_{18}H_{14}$ transform to AFM from the NM state. With the increase of doping level to $x = 2$, both $K_xC_{12}H_{10}$ and $K_xC_{18}H_{14}$

return to the NM state from the AFM state and keep the NM behavior up to $x = 3$. The local spin moment is, respectively, $0.49 \mu_B$ and $0.57 \mu_B$ per formula unit for AFM $K_1C_{12}H_{10}$ and $K_1C_{18}H_{14}$ which are correspondingly larger than those of the edge-shared aromatic compounds. The structural variation is believed as the possible reason of the series of magnetic transitions. For the electronic states at the Fermi level, both $K_xC_{12}H_{10}$ and $K_xC_{18}H_{14}$ exhibit a metallic feature for the doping concentration of $2 \leq x \leq 3$. As a result, we suggest that these NM metallic states are just corresponding to the superconducting phases observed by experiment. Of course, more future efforts are needed to identify every superconducting phase, such as 7.2, 43, and 123 K, in $K_xC_{18}H_{14}$.

ACKNOWLEDGMENT

This work was supported by the Basic Research Program of Shenzhen under Grant JCYJ20160331193059332, Grant JCYJ20150925163313898, Grant JCYJ20150529-143500956, Grant JCYJ20150401145529035, and Grant JCYJ20160331193134437. The work of G.-H. Zhong and H.-Q. Lin was supported in part by the National Natural Science Foundation of China Academy of Engineering Physics under Grant U1530401 and in part by the computational resource from the Beijing Computational Science Research Center. The partial calculation was supported by the Special

Program for Applied Research on Super Computation of the National Natural Science Foundation of China-Guangdong Joint Fund (the third phase) under Grant U1501501.

REFERENCES

- [1] W. A. Little, "Possibility of synthesizing an organic superconductor," *Phys. Rev.*, vol. 134, pp. A1416–A1424, Jun. 1964.
- [2] V. L. Ginzburg, "High-temperature superconductivity—dream or reality?" *Sov. Phys.—Usp.*, vol. 19, no. 2, pp. 174–179, Mar. 1976.
- [3] R. Mitsuhashi *et al.*, "Superconductivity in alkali-metal-doped picene," *Nature*, vol. 464, pp. 76–79, Mar. 2010.
- [4] X. F. Wang *et al.*, "Superconductivity at 5 K in alkali-metal-doped phenanthrene," *Nature Commun.*, vol. 2, no. 1, p. 507, 2011.
- [5] Y. Kubozono *et al.*, "Metal-intercalated aromatic hydrocarbons: A new class of carbon-based superconductors," *Phys. Chem. Chem. Phys.*, vol. 13, no. 37, pp. 16476–16493, 2011.
- [6] M. Q. Xue *et al.*, "Superconductivity above 30 K in alkali-metal-doped hydrocarbon," *Sci. Rep.*, vol. 2, p. 389, Apr. 2012.
- [7] R.-S. Wang, Y. Gao, Z.-B. Huang, and X.-J. Chen. (2017). "Superconductivity in *p*-terphenyl." [Online]. Available: <https://arxiv.org/abs/1703.05803>
- [8] R.-S. Wang, Y. Gao, Z.-B. Huang, and X.-J. Chen. (2017). "Superconductivity at 43 K in a single C-C bond linked terphenyl." [Online]. Available: <https://arxiv.org/abs/1703.05804>
- [9] R.-S. Wang, Y. Gao, Z.-B. Huang, and X.-J. Chen. (2017). "Superconductivity above 120 kelvin in a chain link molecule." [Online]. Available: <https://arxiv.org/abs/1703.06641>
- [10] H. Li *et al.* (2017). "Spectroscopic evidence of low energy gaps persisting towards 120 kelvin in surface-doped *p*-terphenyl crystals." [Online]. Available: <https://arxiv.org/abs/1704.04230>
- [11] W. Liu *et al.*, "Magnetization of potassium-doped *p*-terphenyl and *p*-quaterphenyl by high-pressure synthesis," *Phys. Rev. B, Condens. Matter*, vol. 96, no. 22, p. 224501, 2018.
- [12] G.-H. Zhong, C. Zhong, G.-F. Wu, Z.-B. Huang, X.-J. Chen, and H.-Q. Lin, "First-principles investigations on the magnetic property in tripotassium doped picene," *J. Appl. Phys.*, vol. 113, no. 17, p. 17E131, 2013.
- [13] G. Zhong, Z. Huang, and H. Lin, "Antiferromagnetism in potassium-doped polycyclic aromatic hydrocarbons," *IEEE Trans. Magn.*, vol. 50, no. 11, Nov. 2014, Art. no. 1700103.
- [14] J.-X. Han, G.-H. Zhong, X.-H. Wang, X.-J. Chen, and H.-Q. Lin, "The first-principles investigations on magnetic ground-state in Sm-doped phenanthrene," *AIP Adv.*, vol. 7, no. 5, p. 055704, 2017.
- [15] X.-H. Wang, G.-H. Zhong, J.-X. Han, X.-J. Chen, and H.-Q. Lin, "Structural and antiferromagnetic properties of Sm-doped chrysene," *AIP Adv.*, vol. 7, no. 5, p. 055707, 2017.
- [16] Y. Takabayashi *et al.*, " π -electron $S = 1/2$ quantum spin-liquid state in an ionic polyaromatic hydrocarbon," *Nature Chem.*, vol. 9, pp. 635–643, Apr. 2017.
- [17] J. P. Perdew, K. Burke, and M. Ernzerhof, "Generalized gradient approximation made simple," *Phys. Rev. Lett.*, vol. 77, no. 18, p. 3865, 1996.
- [18] K. Lee, É. D. Murray, L. Kong, B. I. Lundqvist, and D. C. Langreth, "Higher-accuracy van der Waals density functional," *Phys. Rev. B, Condens. Matter*, vol. 82, no. 8, p. 081101, 2010.
- [19] G. Kresse and J. Furthmüller, "Efficiency of *ab-initio* total energy calculations for metals and semiconductors using a plane-wave basis set," *Comput. Mater. Sci.*, vol. 6, pp. 15–50, Jul. 1996.
- [20] G. Kresse and J. Furthmüller, "Efficient iterative schemes for *ab initio* total-energy calculations using a plane-wave basis set," *Phys. Rev. B, Condens. Matter*, vol. 54, no. 16, pp. 11169–11186, 1996.
- [21] G.-H. Zhong *et al.*, "Structural and electronic properties of potassium-doped 1,2;8,9-dibenzopentacene superconductor: Comparing with doped [7]phenacenes," *Mol. Phys.*, vol. 115, no. 4, pp. 472–483, 2017.
- [22] X. Wang, G. Zhong, X. Yan, X. Chen, and H. Lin, "First-principles prediction on geometrical and electronic properties of K-doped chrysene," *J. Phys. Chem. Solids*, vol. 104, pp. 56–61, May 2017.
- [23] G.-H. Zhong *et al.*, "Structural and bonding characteristics of potassium-doped *p*-terphenyl superconductors," *J. Phys. Chem. C*, vol. 122, no. 7, pp. 3801–3808, 2018.
- [24] X. Tian, J. Gu, and J.-B. Xu, "Configuration-dependent electronic and magnetic properties of graphene monolayers and nanoribbons functionalized with aryl groups," *J. Chem. Phys.*, vol. 140, no. 4, p. 044712, 2014.